IceBridge Photon Counting Lidar L1B Subset Geolocated Photon Elevations, Version 1

USER GUIDE

How to Cite These Data

As a condition of using these data, you must include a citation:

Blankenship, D. D., S. D. Kempf, D. A. Young, and L. E. Lindzey. 2012, updated 2014. *IceBridge Photon Counting Lidar L1B Subset Geolocated Photon Elevations, Version 1*. [Indicate subset used]. Boulder, Colorado USA. NASA National Snow and Ice Data Center Distributed Active Archive Center. https://doi.org/10.5067/NR1VABD1ZDTQ. [Date Accessed].

FOR QUESTIONS ABOUT THESE DATA, CONTACT NSIDC@NSIDC.ORG

FOR CURRENT INFORMATION, VISIT https://nsidc.org/data/ILSNP1B

National Snow and Ice Data Center

TABLE OF CONTENTS

1 DATA DESCRIPTION 2
1.1 Parameters 2
1.2 File Naming Convention 2
1.3 Spatial Information 2
1.3.1 Coverage 2
1.3.2 Spatial Resolution 3
1.3.3 Projection and Grid Description 3
1.4 Temporal Coverage 3
1.4.1 Temporal Resolution 3
1.5 Parameter or Variable 3
1.5.1 Parameter Description 3
1.5.2 Sample Data Records 5
2 DATA ACQUISITION AND PROCESSING 5
2.1 Theory of Measurements 5
2.2 Acquisition 7
2.3 Derivation Techniques and Algorithms 7
2.3.1 Trajectory and Attitude Data 8
2.3.2 Error Sources 8
3 SENSOR OR INSTRUMENT DESCRIPTION 8
4 SOFTWARE AND TOOLS 9
5 RELATED DATA SETS 9
6 RELATED WEB SITES 10
7 CONTACTS AND ACKNOWLEDGMENTS 10
7.1 Acknowledgments: 10
8 REFERENCES 10
9 DOCUMENT INFORMATION 11
9.1 Publication Date 11
9.2 Updated Date 11

1 DATA DESCRIPTION

1.1 Parameters

The data files are in HDF5 format. Each data file is paired with an associated XML file. The XML files contain location, platform, and instrument metadata.

1.2 File Naming Convention

The files are named according to the following convention and as described in Table 1:

```
ILSNP1B_2012327_ICP5_JKB2h_F07T02a_005.h5

ILSNP1B_2012327_ICP5_JKB2h_F07T02a_005.h5.xml

ILSNP1B_YYYYDOY_PPP_JKB2h_TTTT_xxx.h5
```

Table 1. Naming Convention

Variable	Description
ILSNP1B	Short name for IceBridge Sigma Space Photon Counting Lidar L1B Time-Tagged Nadir Photon Ranges
YYYY	Four-digit year of survey
DOY	Day of year of survey
PPP	Geographic area (Project)
JKB2h	Host platform for timing (System)
TTTT	Transect name within Project
xxx	Granule within line
.h5	indicates HDF5 file
.h5.xml	indicates XML metadata file

1.3 Spatial Information

1.3.1 Coverage

The target region for this data is East Antarctica, Greenland, and the Antarctic Peninsula. Please see HDF5 metadata for targets for each granule.

Greenland:

Southernmost Latitude 59° N
Northernmost Latitude: 83° N
Westernmost Longitude: 74° W
Easternmost Longitude: 12° W

Antarctica:
Southernmost Latitude: 90° S
Northernmost Latitude: 53° S
Westernmost Longitude: 180° W
Easternmost Longitude: 180° E

1.3.2 Spatial Resolution

10 centimeter spot on the ground at 800 meters (per photon).

1.3.3 Projection and Grid Description

Polar Stereographic at -71 degrees latitude EPSG:3031

1.4 Temporal Coverage

These data were collected as part of ICECAP, NSF, NERC, and Operation IceBridge funded campaigns from 25 November 2010 to the present.

1.4.1 Temporal Resolution

ICECAP campaigns were conducted on an annual basis. East Antarctic campaigns for this data set typically extend from November to early January.

1.5 Parameter or Variable

1.5.1 Parameter Description

Parameters in the HDF5 files are organized as photon data, granule georeferencing data, and transect georeferencing data attributes. In addition, top level attributes store metadata describing platform, beam location on scan, and additional campaign information.

Photon data attributes for BEAM0 through BEAM5 are described in Table 2.

Table 2. Photon Data Attributes

Parameter	Description	Units
DOY	Day Of Year of survey	Day
DScontinuous_time_of_day	Seconds since 2012-12-04 0:0:0	Seconds
DSdelta_time_start	Seconds since 2012-12-04T00:12:03	Seconds
Easting	Apparent projected Easting of photon (WGS-84/ITRF08/EPSG:3031)	Meters
Elevation	Apparent elevation of photon (WGS-84/ITRF08)	Meters
Northing	Apparent projected northing of photon (WGS-84/ITRF08/EPSG:3031)	Meters
X_range_vector	Cross track component of detected surface spot with respect to the lidar body; positive is along right wing	Meters
YEAR	Current year (UTC) (Year of survey)	Year
Y-range_vector	Along track component of detected surface spot with respect to the lidar body; positive is toward nose	Meters
Z-range_vector	Along track component of detected surface spot with respect to the lidar body; positive is down	Meters
cell	Numbered counting channel on detector array	Count
seconds_of_day	Seconds of current day (UTC) (on day of survey)	Seconds

Granule and transect georeferencing data attributes are described in Table 3.

Table 3. Granule and Transect Georeferencing Data Attributes

Parameter	Description	Units
DOY	Day Of Year of survey	Day
DScontinuous_time_of_day	Seconds since 2012-12-04 0:0:0	Seconds
DSdelta_time_start	Seconds since 2012-12-04T00:12:03	Seconds
EW_acceleration	East-West acceleration of the aircraft	Milligal
NS_acceleration	North-South acceleration of the aircraft	Milligal
YEAR	Current year (UTC) (Year of survey)	Year
aircraft_elevation	Elevation of center of gravity GNSS antenna, as determined by real time kalman filter (WGS-84/ITRF08)	Meters
heading_angle	Rotation around aircraft Z axis (with respect to true north, clockwise is positive)	Degrees
latitude	Latitude of laser altimeter spot (WGS-84/ITRF08)	Degrees North
longitude	Longitude of laser altimeter spot (WGS-84/ITRF08)	Degrees East

Parameter	Description	Units
pitch_angle	Rotation around aircraft Y axis (with respect to local geodetic vertical, nose up is positive, zero is aircraft level)	Degrees
position_error	The geometric sum of the expected horizontal and vertical position errors derived by taking the square root of the corresponding Kalman filter variances	Degrees
roll_angle	Rotation around aircraft X axis (with respect to local geodetic vertical, right wing up is positive, zero is wings level)	Meters
seconds_of_day	Seconds of current day	Seconds (UTC)
vertical_acceleration	vertical acceleration of the aircraft	Milliga

1.5.2 Sample Data Records

Below are Elevation values for BEAM1, BEAM2, and BEAM3 from a sample of the ILSNP1B_2012327_ICP5_JKB2h_F07T02a_005.h5 data file as displayed in the HDFView tool.

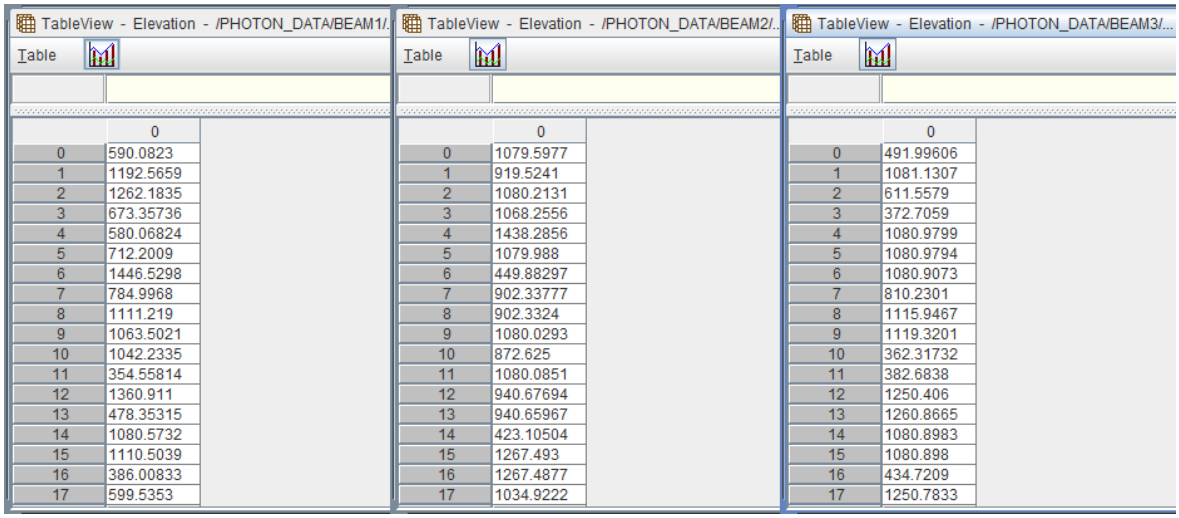

TableView - Elevation - /PHOTON_DATA/BEAM1/

Table

	0
0	590.0823
1	1192.5659
2	1262.1835
3	673.35736
4	580.06824
5	712.2009
6	1446.5298
7	784.9968
8	1111.219
9	1063.5021
10	1042.2335
11	354.55814
12	1360.911
13	478.35315
14	1080.5732
15	1110.5039
16	386.00833
17	599.5353

TableView - Elevation - /PHOTON_DATA/BEAM2/..

Table

	0
0	1079.5977
1	919.5241
2	1080.2131
3	1068.2556
4	1438.2856
5	1079.988
6	449.88297
7	902.33777
8	902.3324
9	1080.0293
10	872.625
11	1080.0851
12	940.67694
13	940.65967
14	423.10504
15	1267.493
16	1267.4877
17	1034.9222

TableView - Elevation - /PHOTON_DATA/BEAM3/...

Table

	0
0	491.99606
1	1081.1307
2	611.5579
3	372.7059
4	1080.9799
5	1080.9794
6	1080.9073
7	810.2301
8	1115.9467
9	1119.3201
10	362.31732
11	382.6838
12	1250.406
13	1260.8665
14	1080.8983
15	1080.898
16	434.7209
17	1250.7833

2 DATA ACQUISITION AND PROCESSING

2.1 Theory of Measurements

The concept of a Photon Counting Lidar (PCL) is described in Degnan, 2002. While the fundamental principles are similar to that of a traditional laser ranging system, a PCL relies on very fast pulse rates and statistical integration to allow detection of lower energy returns, which results in substantial reduction in power, mass, and optical structure requirements. The scanning PCL

system (Degnan et al., 2007) from which the PCL was derived was originally developed as an outer-planets exploration test bed, then adapted for deployment on unmanned airborne vehicles.

The ability to field a light weight instrument with multiple lidar beams was a fundamental driver of the decision to use a photon counting system (the Advanced Topographic Laser Altimeter System, ATLAS) on ICESat-2 (Yu, 2010). The PCL system differs from NASA's Multiple Altimeter Beam Experimental Lidar or MABEL (Brunt et al., 2010), in that the PCL is typically flown at much lower heights (800 meters versus 20,000 m), has more cells (up to 100 versus 16), and actively scans versus having fixed discrete beams.

Our approach to addressing the large data volume involves subsampling the photons into beams chosen to mimic the planned ATLAS configuration, detecting a surface while still in the aircraft-relative frame, and finally georeferencing that surface point.

The objective of beam averaging is to generate a simple data product of manageable volume that can be used both to iteratively determine pointing biases and to accomplish first-order altimetry science goals. To do this we emulate the discrete beams found on the ATLAS system by filtering for photons within limited cones.

For circular scan patterns, we selected six cones within the lidar reference frame sampling the edges, fore and aft, and at 45 degrees. For linear scan patterns, we selected the edges of the scan pattern, the nadir point, and two points in between. Each beam consists of the photons within a single cone. At typical aircraft survey heights, this corresponds to a 10 m wide footprint for each beam. Refer to Figure 1 for locations of geolocated PCL surface recoveries in the Indo-Pacific sector of East Antarctica. Background is bed elevations showing major subglacial basins (Fretwell et al, 2013).

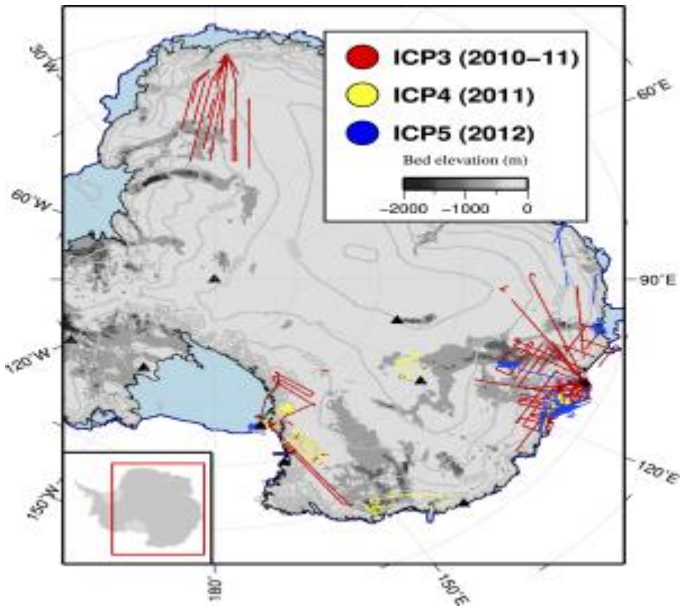

Figure 1. Locations of geolocated PCL surface recoveries in the Indo-Pacific sector of East Antarctica.

2.2 Acquisition

The ICECAP geophysical system was installed on the aircraft at the McMurdo seasonal sea ice runway at the start of each field season. Installation is followed by a calibration flight involving multiple crossovers over flat ice. On typical data-collection flights, the aircraft is flown 600 m to 1000 m above the ground, at a ground speed of 90 m sec-1.

A range gate is applied to limit incoming photons on the PCL. This is adjusted to match the aircraft's height above ice, and was typically 1000 m tall, centered at a distance of 1000 m. Approximately 100 GB of range data are acquired per six hour flight.

2.3 Derivation Techniques and Algorithms

After the trajectory is obtained, for each time step the position and orientation in Earth Centered Earth Fixed space is found, and matrix translations are performed for the sensor lever arm and range vector, following Vaughn et al. (1996) and Koks (2006). The data are then transformed back to the WGS-84 ellipsoidal reference frame.

Pointing biases are determined using an iterative minimization of crossover errors. See Table 4.

Table 4. Pointing Biases

Season	Date	Roll Bias	Pitch Bias	Crossings	Error (cm)	Target
ICP3	December 18, 2010	0.325° (−0.2 25°)	−4.525° (−0.525°)	107 (1976)	10.7 (37)	Law Dome
ICP4	December 23, 2011	0.370° (0.150°)	−4.200° (0.075°)	62 (443)	6.0 (16.9)	McMurdo Ice Shelf
ICP5	November 13, 2012	0.475° (0.175°)	−3.450° (0.025°)	96 (968)	12.5 (23.4)	Ross Ice Shelf

2.3.1 Trajectory and Attitude Data

Please see each granule's HDF5 attributes, and the IPUTG1B dataset for details of trajectory collection.

2.3.2 Error Sources

The lidar coarse clock used to calculate ranges has a temperature and acquisition card dependent uncertainty of 0.1 percent, which translates to a scaling error in range of ~80 cm. For this reason, we use the ILUTP2 data to calibrate results in the Elevation and Slope section of the ILSNP4 data set.

GPS relative errors are estimated by Waypoint to be typically 6 cm where a convergent combined GPS-IMU solution is produced, with orientation errors of 50 µrad.

For 2010-11 data, GPS errors were higher (typically 10 cm) as the GPS data was not constrained by IMU data.

We used a simple, static 1-D atmospheric model to estimate delays due to propagation through air.

3 SENSOR OR INSTRUMENT DESCRIPTION

In the Photon Counting Lidar (PCL) system a 532 nm laser beam, pulsed at ~19 kHz, is split into a 10 x 10 grid of beamlets and projected through a Risley prism beam steering unit, with time of the outgoing pulse recorded as the pulse start. The angular spread of the beamlets is 0.12° along each side of the grid yielding an illuminated grid on the ground of about 1-2 meters for every shot.

For the 2010-11 season, two prisms were used to generate a 45 degrees linear scan pattern, with a maximum deflection from nadir of 14.9 degrees. During the 2011 and 2012 seasons only one prism was used, which resulted in a reduced circular scan pattern with 7.3 degrees deflection from nadir. The beam steering unit is synchronized to the laser, such that one cycle of the beam steering

unit corresponds to 1024 shots after the system has spun up after starting; thus the system scans underlying terrain at 18.5 Hz. Return photons are received through the same optics and directed to a 10 x 10 cell anode microchannel plate photomultiplier. Timing of the returns is split 50/50 between two independent Field-Programmable Gate Arrays (FPGAs).

Each cell has a coarse, 16 bit approximately 295 Hz clock (range resolution ~0.5 meters) and a fine 8 bit ~12.5 GHz clock (range resolution ~1.2 cm), calibrated per shot that allows ~0.1 nsec precision for detection times (stops). The differences between the starts and stops is the time of flight, which multiplied by an appropriate velocity of light provides the apparent range to the photon source. The coarse clock rate can drift due to temperature and hardware issues by up to 0.01 percent, limiting absolute accuracy to 80 cm without registration to the LAS.

The 0.7 nsec pulse width limits the precision of start times, yielding a minimum range precision per-photon of ~10.5 cm. Systematic biases between individual cells are estimated to be symmetrically distributed with a root mean squared (RMS) deviation of 15 cm. Higher precision requires stacking numerous individual shots.

Time stamps are generated with every shot, every prism rotation, and on reception of a 1 Hz GPS generated pulse from timing calibration. The timing data from each FPGA is recorded directly to independent hard drives, typically at 4-5 MB sec-1. In post-processing, these time stamps allow each photon's time-of-flight to be converted into an X, Y, and Z location relative to the sensor.

4 SOFTWARE AND TOOLS

The following external links provide access to software for reading and viewing HDF5 data files. Please be sure to review instructions on installing and running the programs. Version 1.8.5 of the HDF5 libraries was used.

HDFView: Visual tool for browsing and editing HDF4 and HDF5 files.

h5py: Free python module for interacting with HDF5 data. Depends on the SciPy/NumPy suite of Python Modules.

Matlab: The h5read command in recent versions of Mathworks Matlab can also access HDF5 variables.

For additional tools, see the HDF-EOS Tools and Information Center.

5 RELATED DATA SETS

- IceBridge Sigma Space Prototype L0 Raw Time-of-Flight Data

- IceBridge Sigma Space Lidar L0 Raw Time-of-Flight Data
- IceBridge Sigma Space Photon Counting Lidar L2 Geolocated Nadir Photon Elevations
- IceBridge GPS/IMU L1B Primary Position and Attitude Solution

6 RELATED WEB SITES

- IceBridge Product Web Site
- IceBridge Web site at NASA
- ICESat/GLAS Web site at NASA Wallops Flight Facility
- ICESat/GLAS Web site at NSIDC
- University of Texas Institute for Geophysics Web site

7 CONTACTS AND ACKNOWLEDGMENTS

Donald D. Blankenship, Duncan A. Young, Laura E. Lindzey, Scott D. Kempf

University of Texas at Austin

Institute for Geophysics

Austin, TX, 78759-8500

7.1 Acknowledgments:

ICECAP/Operation Ice Bridge. See each granule HDF5 metadata for specific grants and logistical support.

8 REFERENCES

Brunt, K. M., H. A. Fricker, L. Padman, T. A. Scambos, and S. O'Neel. 2010. Mapping the Grounding Zone of the Ross Ice Shelf, Antarctica, Using ICESat Laser Altimetry, Annals Of Glaciology, 51(55):71-79, doi:10.3189/172756410791392790.

Degnan, J., D. Wells, R. Machan, and E. Leventhal. 2007. Second Generation Airborne 3D Imaging Lidars Based on Photon Counting, SPIE Proceedings: Lidar, 6771/67710N. 10.1117/12.732086.

Degnan, J. J. 2002. Photon-counting Multikilohertz Microlaser Altimeters for Airborne and Spaceborne Topographic Measurments, Journal Of Geodynamics, 34(3-4): 503-549.

Fretwell, P., et al. 2013. Bedmap2: Improved Ice Bed, Surface and Thickness Datasets for Antarctica, The Cryosphere, 7: 375--393, 10.5194/tc-7-375-2013.

Koks, D. 2006. Using Rotations to Build Aerospace Coordinate Systems, Australian Government, Defence Science and Technology Organization, DSTO-TN-0640.

Vaughn, C. R., J. L. Button, W. B. Krabill, and D. Rabine. 1996. Georeferencing of Airborne Laser Altimeter Measurements, International Journal Of Remote Sensing, 17, 11, 2185-2200, 10.1080/01431169608948765.

Young, D. A., et al. In review. Extending Surface Elevation Time Series in East Antarctica Using ICECAP Photon Counting Swath Altimetry, Journal Of Glaciology.

Yu, A. W., et al. 2010. Space Laser Transmitter Development for ICESat-2 Mission, Proceedings Of SPIE, 7578, 757809-2.

9 DOCUMENT INFORMATION

9.1 Publication Date

25 June 2014

9.2 Updated Date

06 August 2015